www.czasopisma.pan.pl PAN POLSKA AKADEMIA NAUK www.journals.pan.pl

Arch. Metall. Mater. **70** (2025), 4, 1585-1593

DOI: https://doi.org/10.24425/amm.2025.156238

M.M. KARAŚ[1], M. BIEDA[2*], Ł. MAJ[2], S. BOCZKAL[1], A. JARZĘBSKA[2], Z. ZAJĄC[2], B. AUGUSTYN[1], D. KAPINOS[1], K. LIMANÓWKA[1], J. SKIBA[3]

AN ALTERNATIVE APPROACH FOR PRODUCING ELECTROLYTIC COATINGS TO ENHANCE CORROSION RESISTANCE OF BIODEGRADABLE MAGNESIUM ALLOY

A protective coating was developed on a biodegradable MgZn1Ca0.2Li1 alloy via micro-arc oxidation (MAO) method in a KOH + KF electrolyte. The coating, composed of MgF_2, $KMgF_3$, and MgO phases, uniformly covers the substrate material, exhibiting moderate surface roughness. Comprehensive analysis using XRD along with scanning and transmission electron microscopy cross-sectional observations, supported by the acquisition of diffraction patterns and EDS spectra, was conducted to confirm the nanocrystalline structure as well as the phase and elemental distribution. Electrochemical tests showed a tenfold decrease in corrosion current and a significant increase in polarization resistance. Hydrogen evolution was effectively suppressed, confirming protective barrier function. The use of environmentally friendly KOH and KF-containing electrolyte ensures the non-toxicity of the deposition process, resulting in the protection of future biodegradable implant surfaces. The results support the potential of this coating for orthopedic applications.

Keywords: Magnesium alloys; micro-arc oxidation; microstructure; corrosion resistance; hydrogen evolution

1. Introduction

Biodegradable materials have gained a significant importance in the design of bone implants, providing temporary mechanical support and the ability to integrate with natural tissue. Their application in orthopedics helps to reduce the complications typical for permanent implants, including chronic inflammation and stress shielding, while simultaneously supporting osteoregeneration. To be suitable for bone-related applications, these materials must exhibit biocompatibility, appropriate degradation rate, sufficient mechanical properties and the capacity to support osteoconduction and osteointegration [1]. Magnesium and its alloys, presenting a low density and Young modulus compatible with bone (minimizing the risk of bone resorption), are the most extensively studied group of biodegradable materials. In addition, magnesium, as a natural physiological component, demonstrate high biocompatibility and supports osteogenesis [2]. Despite these beneficial properties, magnesium is characterized by a high electrochemical potential (~ –2.4 V), which leads to rapid corrosion involving anodic dissolution and cathodic water decomposition with hydrogen evolution. Corrosion products can compromise biocompatibility and hinder tissue integration. In alkaline environments, protective layers are formed, however, the presence of Cl^- anions destabilizes them, accelerating degradation [3]. In order to improve these drawbacks, the strategy covering addition of alloying elements [4] and/or the formation of protective coatings have been introduced [5]. The introduction of alloying elements requires careful toxicological assessment, as some of them, such as popular aluminum or rare earth elements, may exert a harmful effect on the body [6]. Therefore, alloying additions such as calcium and zinc, gained a significant popularity. Calcium (Ca), a natural bone component, supports tissue regeneration by stimulating osteoclasts and osteoblasts. When added to magnesium alloys, it improves both corrosion resistance and mechanical strength [7]. Zinc (Zn) enhances enzyme function while improving mechanical parameters, biocompatibility, and corrosion resistance [8]. Moreover, the addition of lithium (Li) improves the plasticity of magnesium alloys, stabilizes the degradation rate, and reduces hydrogen evolution during corrosion [9]. The Mg-Zn-Ca-Li alloy demonstrates numerous advantages over traditional magnesium alloys, making it particularly attractive for use in biodegradable medical implants.

[1] ŁUKASIEWICZ RESEARCH NETWORK – INSTITUTE OF NON-FERROUS METALS LIGHT METALS DIVISION IN SKAWINA, POLAND
[2] INSTITUTE OF METALLURGY AND MATERIALS SCIENCE, POLISH ACADEMY OF SCIENCES, KRAKÓW, POLAND
[3] INSTITUTE OF HIGH PRESSURE PHYSICS, POLISH ACADEMY OF SCIENCES, WARSAW, POLAND

* Corresponding author: m.bieda@imim.pl

Due to the need to improve degradation behavior and limit hydrogen release, the application of protective coatings is still essential.

Deposition of protective coatings was already suggested to control the degradation rate of magnesium-based biomaterials as well as to adjust the kinetics of hydrogen evolution. The goal is to synchronize the material's resorption with the physiological timeline of bone healing. Additionally, such coatings enhance the biocompatibility of the implant surface by minimizing inflammatory responses and supporting osteointegration and bone regeneration. Especially, MgF_2-rich coatings play a key role in corrosion protection under physiological conditions by reducing corrosion current density, shifting corrosion potential, and suppressing hydrogen evolution and pH elevation. It also enhances cytocompatibility by moderating the release of Mg^{2+} ions and promoting osteoblast adhesion and proliferation [10]. The chemical conversion coating (CCC) technique, often involving HF-based acidic solutions (e.g., HF with H_3PO_4 or HNO_3) [11-13], enables the rapid formation of MgF_2-rich layers without requiring an external power source. However, this method is associated with substantial toxicological and environmental risks due to the high corrosivity of HF and the challenges in waste disposal. Moreover, coatings produced by CCC tend to be thinner, less adherent, and structurally non-uniform, which limits their long-term corrosion protection capabilities.

A focus on conversion coatings, produced through chemical reactions between the magnesium substrate and the electrolyte was placed in recent studies on development of coating methods of Mg-based alloys. The microstructure and functional properties of these coatings depend significantly on the composition of the alloy, the electrical parameters and selection of the electrolyte [14]. In this way, high-voltage micro-arc oxidation (MAO) method is intensively developed, the forming thick (10-50 µm), porous, and well-adherent oxide layers. Electrolytes typically used in MAO include phosphate-, silicate-, and fluoride-based solutions, which facilitate the formation of ceramic coatings with excellent corrosion and wear resistance [10,15,16]. In the MAO process, high voltage promotes intensive surface oxidation, leading to the formation of substantial amounts of MgO as the dominant component of the oxide layer. In addition, despite its advantages, standard MAO process involves the use of high voltages (up to 600 V) and is characterized by intense plasma discharges, requiring advanced equipment and precise control of process parameters. On the other hand, traditional anodizing, conducted at significantly lower voltages (15-50 V), produces coatings with longer processing times. Therefore, more efficient methods of MgF_2-based conversion coatings need to be developed.

The present study investigates the properties of a conversion coating produced by micro-arc oxidation in a highly-concentrated KOH + KF electrolyte, applied to the biodegradable as-cast MgZn1Ca0.2Li1 alloy. The objective was to develop a protective coating capable of reducing the corrosion rate and hydrogen evolution under physiological conditions while maintaining a controlled degradation rate. The coating was analyzed with respect to its microstructure, phase/chemical composition, and corrosion behavior under simulated physiological conditions in order to demonstrate its effectiveness.

2. Materials and Methods

Samples of the MgZn1Ca0.2Li1 alloy were produced by gravity die casting in an Ar + SF_6 atmosphere. The chemical composition was determined using an optical emission spectrometer (OES, ARL 4460) and atomic absorption spectroscopy (AAS) and presented in TABLE 1.

TABLE 1

The chemical composition of magnesium alloy

Contents, % by weight			
Zn [%]	Ca [%]	Li [%]	Mg [%]
0.95	0.22	0.92	Remaining

The micro-arc oxidation (MAO) was performed with an electrolyte composed of 80 g/l KOH and 300 g/l KF with the use of technological setup schematically presented in Fig. 1a. The magnesium alloy sample acted as the anode, and a stainless steel electrode served as the cathode. The coating was produced under the constant current density of 10 A/dm^2 (galvanostatic mode), processing time of 5 min, and solution temperature of 25°C.

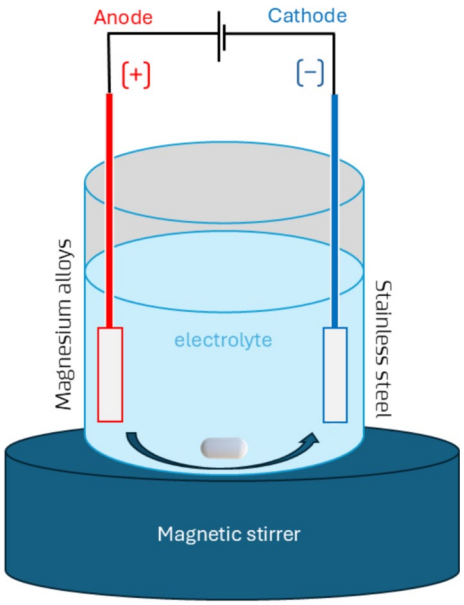

Fig. 1. Schematic diagram of the process

The measurement of the coating thickness was performed using the ImageJ software. A total of 60 measurements were taken on SEM/BSE images. Based on these measurements, the coating thickness, standard deviation, minimum value, and maximum value were calculated. Quantitative analysis of the surface topography was carried out using a Zeiss Smartzoom 5 automated digital microscope. Roughness parameters were determined according to ISO 25178 using Zeiss ConfoMap software. The

phase composition of the coatings was identified using X-ray diffraction (XRD) method and Bruker D8 Discover diffractometer equipped with Cu anode. Data was analyzed with Diffrac.EVA 3.0 and HighScore Plus 4.8 software, using the ICDD PDF-4+ database of crystallographic compounds. The cross-sectional studies were performed with scanning electron microscopy (SEM, FEI Quanta 3D, FEG). Electron-backscattered diffraction (EBSD) in SEM was applied for orientation mapping of the substrate material. Specimens for transmission electron microscopy (TEM) were prepared using a focused ion beam (FIB, DualBeam ThermoFisher Scios 2), and observations were carried out using a ThermoFisher Themis microscope (200 kV, FEG) equipped with EDAX energy-dispersive X-ray spectrometer (EDS). To evaluate corrosion resistance, electrochemical tests were conducted, including 1-hour open-circuit potential (OCP) stabilization measurements (AUTOLAB PGSTAT 302, Ringer Solution at 37°C, pH 7.4), as well as immersion tests in Hank's Balanced Salt Solution (HBSS) for 7 days at 37°C and pH of 6.9 ± 0.2. Corrosion rates were calculated based on mass loss and electrochemical parameters. The corrosion rate was derived from potentiostat data using standard calculation formulas.

$$R = K\frac{J_{corr}}{\rho}me,\ m_e = \frac{M}{n\cdot F}$$

R – corrosion rate [mm/year],
$K = 3{,}27 * 10^3$ [mm·g/(C·cm·year)] – empirical constant,
J_{corr} – corrosion current density [A·cm^{-2}],
ρ – density of the material [g/cm^3],
m_e – stoichiometric equivalent [u],
M – molar mass of the metal [g/mol],
n – number of electrons exchanged in the electrochemical reaction,
F – Faraday's constant (96,485 C/mol).

Hydrogen release was monitored using a setup consisting of a graduated cylinder and an Erlenmeyer flask filled with Ringer's solution, incubated at 37°C. Corrosion products were assessed based on the volume of released H_2, according to the following reactions:

- Anodic reaction:

$$Mg(s) \rightarrow Mg^{2+}(aq) + 2e^- \quad (1)$$

- Cathodic reaction:

$$2H_2O(aq) + 2e^- \rightarrow 2OH^-(aq) + H_2(g) \quad (2)$$

- Overall reaction:

$$Mg(s) + 2H_2O(aq) \rightarrow Mg(OH)_2(s) + H_2(g) \quad (3)$$

- Secondary reaction with chloride ions:

$$Mg(OH)_2(s) + 2Cl^-(aq) \rightarrow MgCl_2 + 2OH^-(aq) \quad (4)$$

The released hydrogen was collected in an inverted graduated cylinder. As the hydrogen gas accumulated, it displaced the water inside the cylinder, allowing for daily quantification of the hydrogen volume evolved from the magnesium sample.

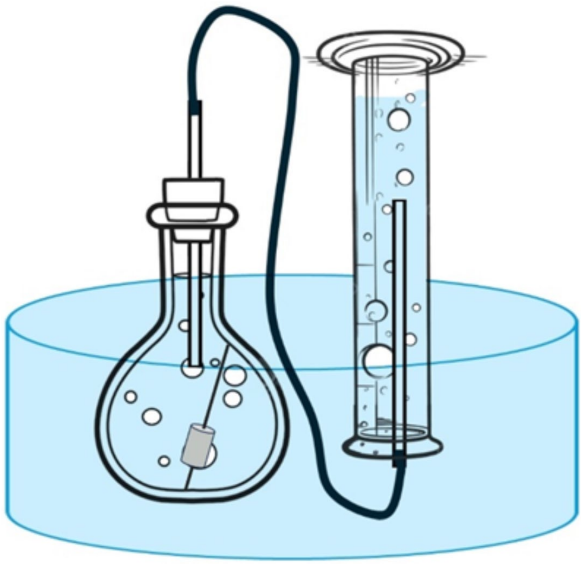

Fig. 2. Scheme of hydrogen evolution measurement setup and experimental station for hydrogen release testing

3. Results

The micro-arc oxidation (MAO) process was performed in the way to maintain constant current density of 10 A/dm^2. Registered changes in voltage values (in the function of processing time) are shown in Fig. 3. During the first several seconds after the start of the deposition process, a steep but linear increase in voltage occurs, corresponding to typical anodization process. After reaching ~35 V, sparking starts to occur and the voltage tends to slowly increase and stabilize at the level of ~70 V. For the longer processing times, larger oscillations of the voltage values may be noticed, connected with formation of more intense discharges.

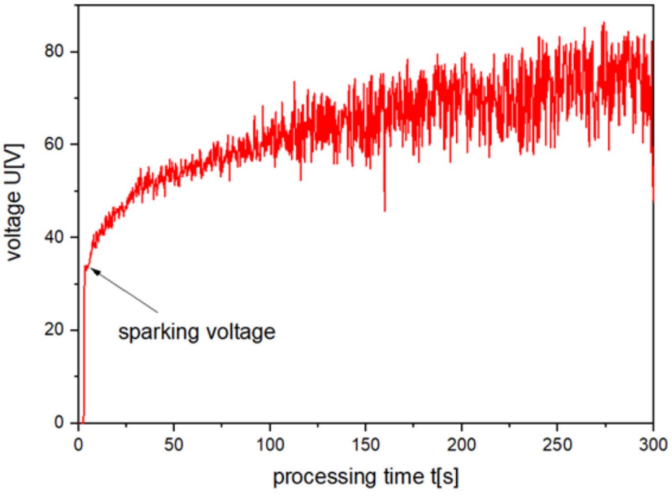

Fig. 3. Voltage vs processing time curve registered during micro-arc oxidation

The microstructure and chemical composition of the as-cast MgZn1Ca0.2Li1 alloy, being the substrate for micro-arc

oxidation, were examined using SEM/EBSD and SEM/EDS methods, respectively (Fig. 4). The SEM/BSE images revealed the presence of grains of the Mg-rich matrix as well precipitates at the grain boundaries. The EDS spectra showed distinct peaks corresponding to the presence of magnesium, zinc and calcium (the presence of Li was not confirmed with EDS due its low Z number). The orientation maps analysis of both cross-sections revealed an coarse-grained microstructure with large grain size with nearly random orientation suggesting a weak texture of the material. Uniform coloring of the orientation maps suggests a lack of substructure and defects.

The XRD spectrum of coated MgZn1Ca0.2Li1 alloy is presented in Fig. 5. It reveals the presence of diffraction peaks corresponding to Mg, MgO, MgF_2, and $KMgF_3$ phases, confirming crystalline nature of the coating. The Mg signal originates from the substrate. A semi-quantitative analysis of phase content indicated that the total amount of fluoride phases exceeds that of the oxide phase with MgO content lower than 40 wt.% (TABLE 2).

The surface morphology of the coating was analyzed qualitatively and quantitatively by means of SEM/SE plan-view observations and surface analysis with digital microscope, respectively (Fig. 6). The SEM/SE image of the sample surface revealed an irregular morphology with considerably high hillocks and valleys. Highly developed surface of the coating was also confirmed with a surface topography mapping (with color gradients corresponding to different height levels – from blue (lowest) to red and white (highest) – with a vertical range reaching up to 28 µm). A three-dimensional reconstruction of the same surface topography is also included (Fig. 6c). In that way, relatively considerable values of parameters of S_x and S_a were confirmed i.e. 24.1 µm ± 8.37 µm and 4.8 µm ± 0.74 µm . The cross-sectional SEM/BSE (Fig. 6b) studies revealed a porous structure with irregular voids and inhomogeneities, even if relatively uniform

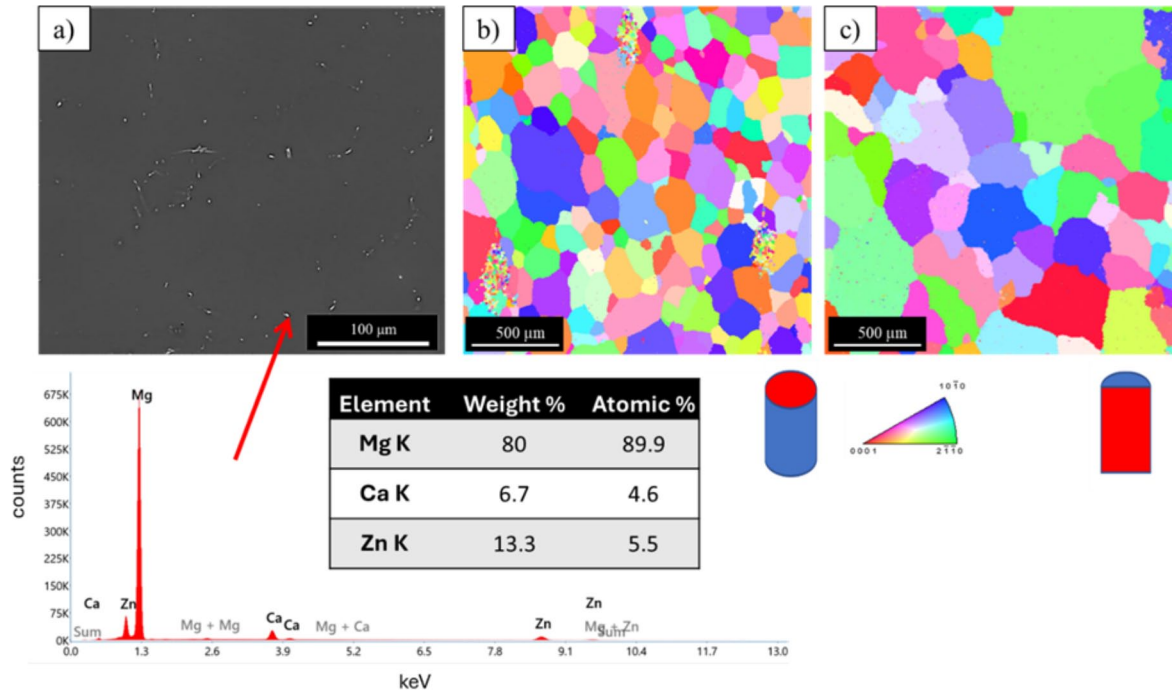

Fig. 4. SEM/BSE image with exemplary EDS spectrum a), and SEM/EBSD orientation maps of the MgZn1Ca0.2Li1 from cross sections of the as-cast ingot b), c)

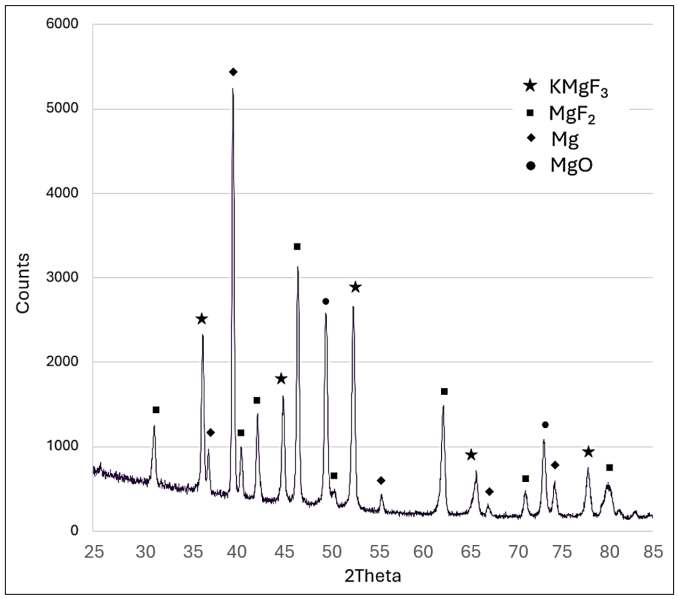

Fig. 5. XRD diffraction pattern of the MgZn1Ca0.2Li1 alloy with conversion coating

TABLE 2

Percentage content of phases present in the conversion coating

Phase, [-]	Percentage content, [wt.%]
MgO	39.7
MgF_2	28.7
$KMgF_3$	31.6

coverage of the substrate was obtained. The larger porosity was confirmed to develop mainly in the bottom parts of the coating, close to the interface with the substrate material, while smaller ones were randomly dispersed throughout the whole coating. The measured coating thickness from cross-sectional BSE images varied between approximately 8.6 µm and 26.9 µm, with an average thickness of about 16 µm ± 4.1 µm.

SEM/EDS elemental mapping confirmed the presence and distribution of magnesium (Mg), fluorine (F), and potassium (K) within the coating (Fig. 7). The coating present detectable levels of oxygen (O), but its distribution was not effectively demonstrated. A uniform distribution of fluorine and magnesium can be observed throughout the entire coating, whereas potassium appears in the form of localized clusters, primarily near the surface of the coating.

TEM/BF cross-sectional observations confirmed fully crystalline microstructure of the coating presenting an ultrafine-grained nature with cracks and nanoporosity. The obtained EDS maps (Fig. 8) revealed the distribution of magnesium, fluorine, potassium, and oxygen within the coating. Magnesium and fluorine were relatively uniformly distributed throughout the layer. Potassium appeared locally, primarily near the outer surface of the coating, while oxygen was evenly dispersed across the entire structure. To confirm the phase distribution throughout the coating, phase analysis, basing on indexation of selected area electron diffraction (SAED) patterns, was also performed (Fig. 9), con-

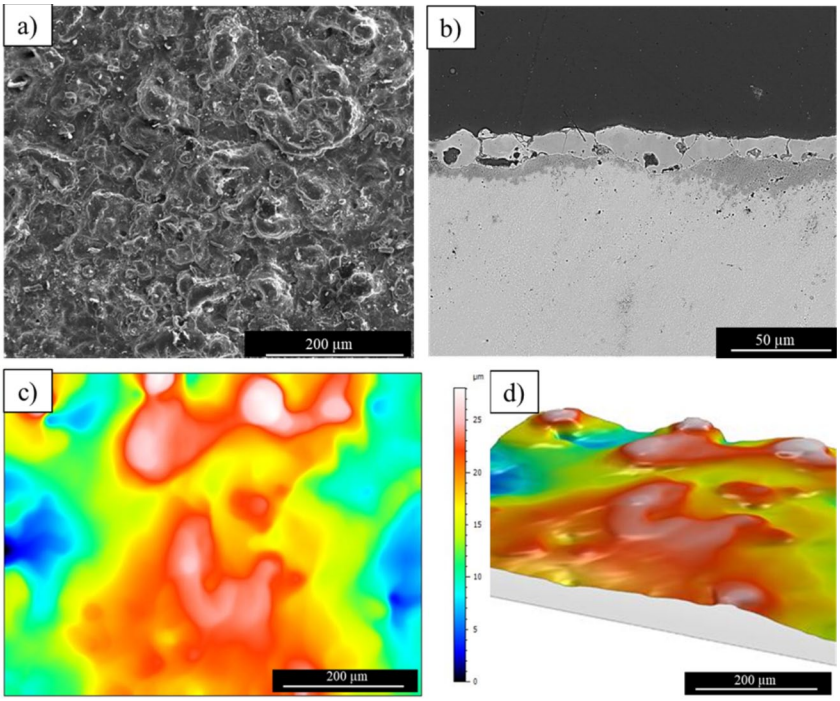

Fig. 6. SEM/ SE images of the surface a) and SEM/ BSE image of the cross-section b) of the coating produced on MgZn1Ca0.2Li1 alloy; 2D and 3D images of surface roughness c),d) respectively

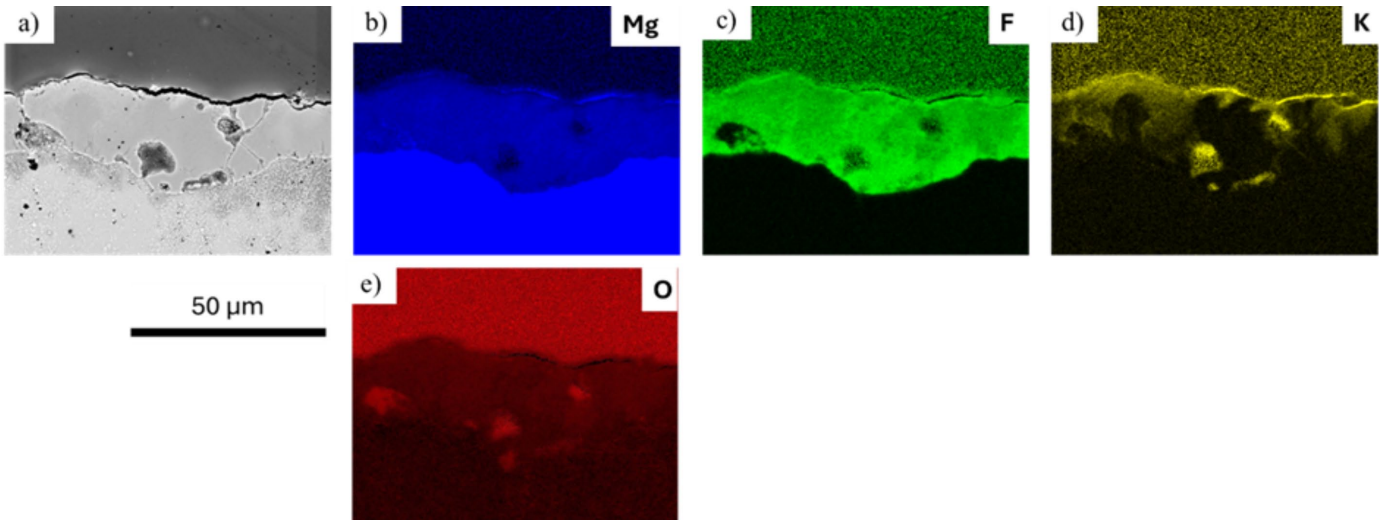

Fig. 7. SEM/EDS analysis of the conversion coating: a) SEM/BSE cross-sectional image of the analyzed area, b) magnesium, c) fluorine, d) potassium, e) oxygen

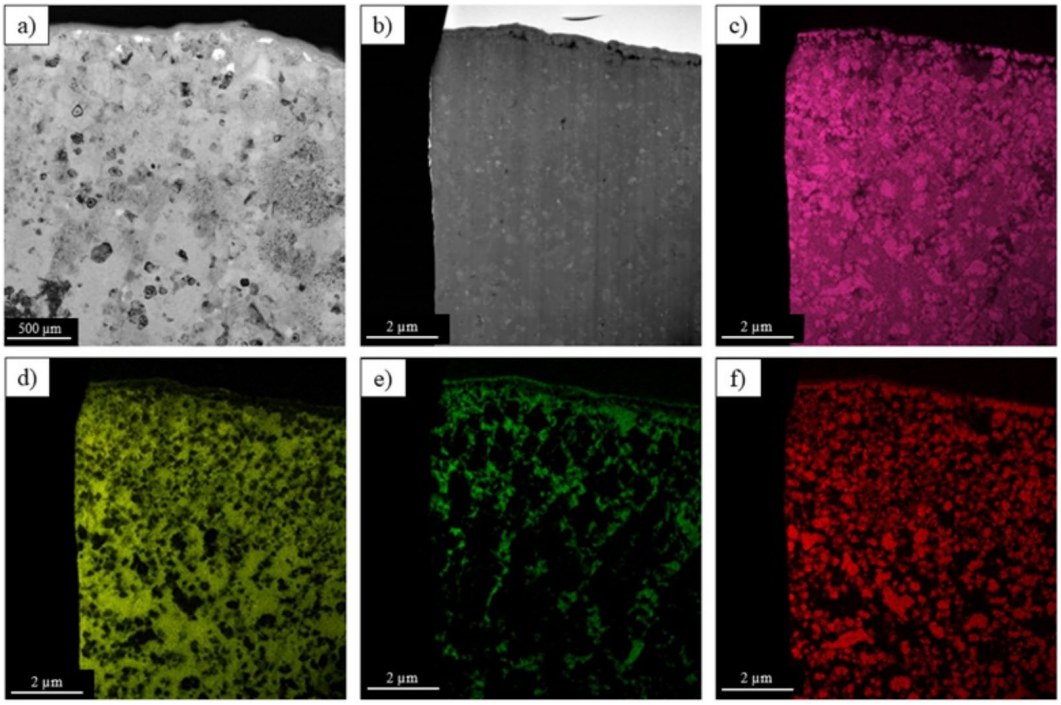

Fig. 8. TEM analysis of the micro-arc oxidation coating produced on MgZn1Ca0.2Li1 alloy:a) TEM/BF microstructure image, (b) STEM image and EDS maps of c) magnesium, d) fluorine, e) potassium, f) oxygen

firming the presence of phases such as $KMgF_3$, MgF_2, and MgO. MgO oxides nanograins are uniformly dispersed throughout the MgF_2 matrix, while $KMgF_3$ was confirmed mainly in the upper parts of the coating.

To assess the electrochemical properties, polarization curves were analyzed (Fig. 10). The corrosion potential (E_{corr}) shifted from –1547 mV to –1439 mV, while the corrosion current density (I_{corr}) decreased from 5.1×10^{-5} A/cm^2 to 9.32×10^{-6} A/cm^2. The polarization resistance (R_p) increased from 340 Ω to 3428 Ω. Those values indicate enhanced resistance to electrochemical corrosion. The uncoated sample exhibited a calculated corrosion rate of 1.28 mm/year, whereas the sample with the conversion coating showed a significantly reduced corrosion rate of 0.14 mm/year.

Based on the measurements of hydrogen release from coated and uncoated samples, a graph was plotted showing the relationship between hydrogen evolution and exposure time for 28 days of immersion (Fig. 11). Uncoated samples (black markers) show an exponential increase in hydrogen evolution after

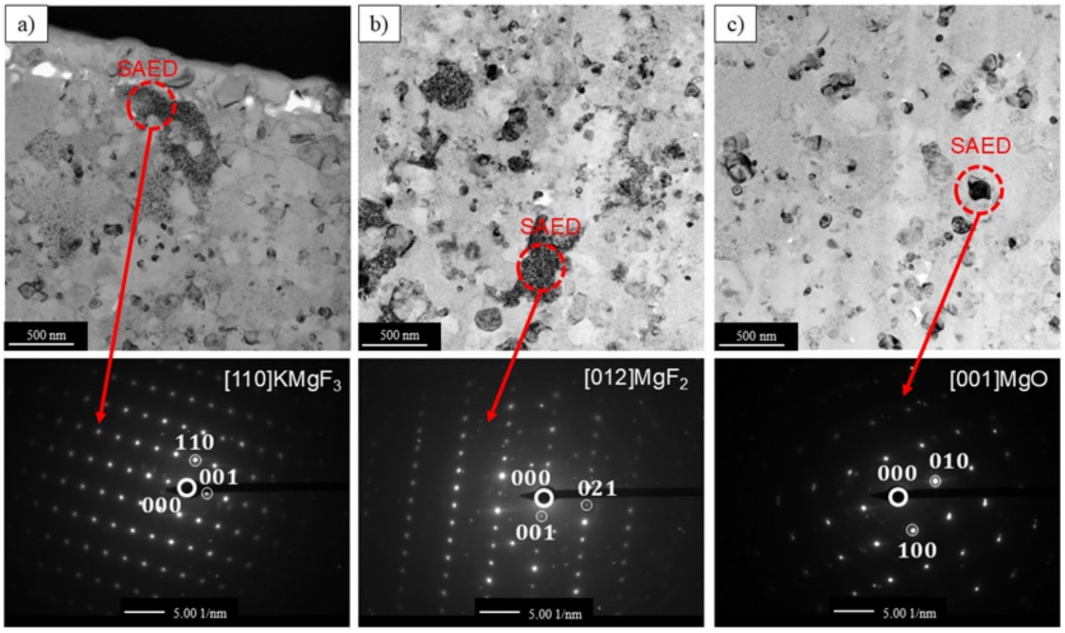

Fig. 9. TEM/BF microstructure images and the corresponding SAED patterns acquired from the conversion coating for a) $KMgF_3$, b) MgF_2 and c) MgO respectively

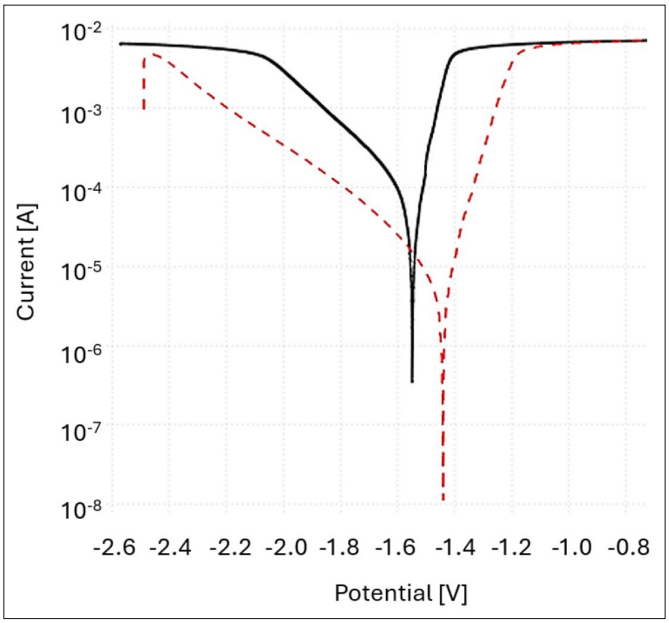

Fig. 10. Comparison of polarization curves for the uncoated alloy (black) and the alloy with a conversion coating (red)

about 10 days, reaching over 65 mL/cm^2 by day 28th, indicating an intense corrosion activity. In contrast, coated samples (red markers) maintain consistently low hydrogen release throughout this period. In Fig. 11b one may notice that bare substrate subjected to immersion test presents evident both localized corrosion with the areas having large pits (corresponding to the sharp increase in hydrogen evolution in Fig. 11a) as well as nearly unaffected, flat regions. On the other hand, uniform corrosion with invisible pitting was confirmed for sample with micro-arc oxidation coating.

4. Discussion

In this work, the highly concentrated KOH + KF electrolyte was used for micro-arc oxidation of the MgF_2-based conversion coating on as-cast Mg-based alloy. This solution enabled the formation of a coating with dominant fluoride phases as well as with appropriate thickness and porosity, being difficult to achieve using other electrolytes [17]. In addition, KOH + KF is non-toxic and alkaline, making the process inherently safer compared to more aggressive chemistries (e.g., hydrochloric acid-based systems), as noted in other studies [18]. This also contributes to the environmental friendliness of the coating process.

The analysis of the surface topography confirmed a moderate roughness (Sa = 4.2±0.4 µm) as well as the presence of the porosity of the as-deposited coatings. It is favorable from the point of view of acceleration of osteointegration as the former studies emphasize that the surface roughness in the range of 1-5 µm is optimal for osteoblast adhesion and proliferation, as well as for establishing a strong bone-implant interface [19]. It was also already shown that porous coatings with controlled roughness can facilitate both osteointegration and the diffusion of bioactive substances [20].

The microstructure and phase analysis of the as-deposited coating confirmed the presence of three phases: MgO, MgF_2, and $KMgF_3$. Formation stages and corresponding chemical reactions are presented below:

Step 1. Electrolyte dissociation in aqueous solution:

$$KF \rightarrow K^+ + F^- \quad (1)$$

$$KOH \rightarrow K^+ + OH^- \quad (2)$$

Step 2. Anodic oxidation of magnesium to Mg^{2+} and formation of $Mg(OH)_2$ and MgO:

$$Mg \rightarrow Mg^{2+} + 2e^- \quad (3)$$

$$Mg^{2+} + 2OH^- \rightarrow Mg(OH)_2 \quad (4)$$

$$Mg(OH)_2 \rightarrow MgO + H_2O$$
(at high plasma temperatures due to the sparking) (5)

Step 3. Formation of magnesium fluoride:

$$Mg^{2+} + 2F^- \rightarrow MgF_2 \quad (5)$$

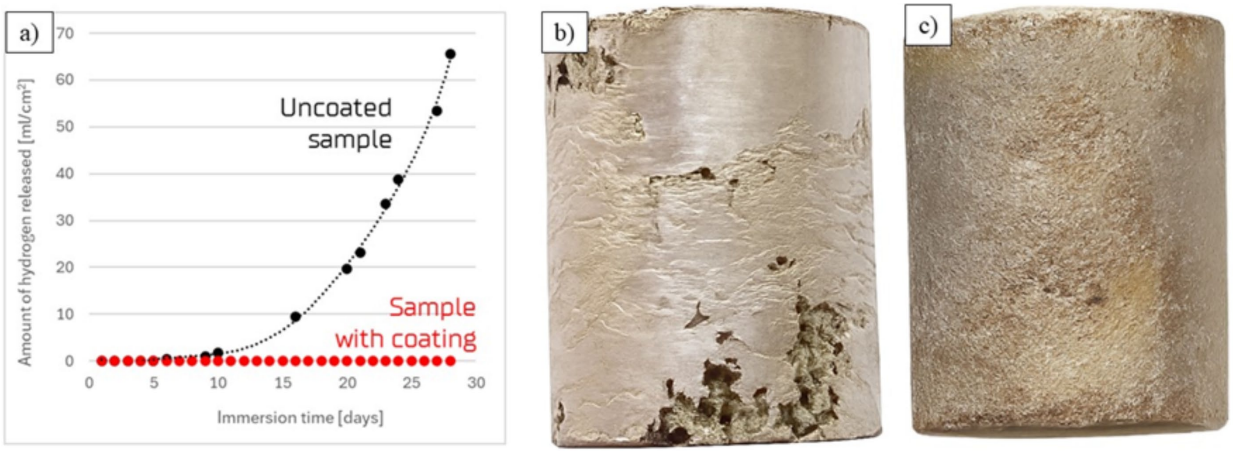

Fig. 11. The graph presenting comparison of hydrogen evolution during incubation of uncoated and conversion-coated samples a) and the images of the sample after the immersion test: b) sample without coating and c) sample with coating after 28 days in immersion corrosion test

Step 4. Formation of $KMgF_3$ phase:

$$K^+ + Mg^{2+} + 3F^- \rightarrow KMgF_3 \quad (6)$$

This reaction may occur directly within the micro-arc plasma region on the anodic surface, where local thermal conditions (exceeding 2000 °C) favor the crystallization of phases with low formation enthalpy [13]. In this way, favorable, fluoride-rich microstructure was formed. Both magnesium oxide and magnesium fluoride are known for their high chemical resistance and surface passivation capabilities [21]. Coatings containing MgF_2 and $KMgF_3$ reduce the corrosion current density by up to an order of magnitude compared to uncoated materials [19]. Our approach showed that, in contrary to other techniques of fabrication of MgF_2 coatings, micro-arc oxidation in highly concentrated KOH + KF solution is less time consuming and avoid using of hazardous chemicals such as hydrofluoric acid [22].

The obtained results of electrochemical tests confirm the effectiveness of the conversion coating in improving the corrosion resistance of the biodegradable MgZn1Ca0.2Li1 alloy. An increase in polarization resistance from 340 Ω to 3428 Ω, along with a decrease in corrosion current density from 5.1×10^{-5} A/cm^2 to 9.32×10^{-6} A/cm^2, indicates a reduction in anodic dissolution and improved electrochemical stability in a simulated physiological environment. The results of previous studies showed that the effectiveness of protective coatings in mitigating magnesium corrosion degradation depends primarily on their compactness and chemical composition [23].

Hydrogen evolution determined through the immersion test represents an important functional evaluation method for magnesium-based implants. Excessive hydrogen evolution in vivo may lead to the formation of gas pockets in tissue, potentially causing inflammation and delayed osteointegration [24]. The conversion-coated samples showed no hydrogen release and more uniform behavior (compare to uncoated samples) of degradation process during the entire incubation period, indicating effective protection of the biomaterial.

5. Conclusions

In this work, the MgZn1Ca0.2Li1 alloy produced by gravity die casting was subjected to low-voltage micro-arc oxidation in highly concentrated KOH+KF electrolyte. The studies of surface topography, microstructure, electrochemical tests as well as immersion tests focused on hydrogen evolution allowed to conclude that:

- As-cast MgZn1Ca0.2Li1 alloy exhibits a uniform, coarse-grained and defect-free microstructure with equiaxed grains of Mg matrix and Ca-/Zn-rich precipitates on grain boundaries, and its elemental composition corresponds to the designed concentrations of Zn, Ca, and Li, providing a suitable basis for subsequent surface modification.
- The micro-arc oxidation carried out in constant current mode with the use of highly-concentrated, non-toxic KOH + KF electrolyte allowing to significantly decrease its conductivity and, in this way, to reduce the sparking voltage down to ~35 V and stabilize the processing voltage at ~70 V, confirmed the possibility of producing a conversion coating at low-voltage conditions
- The coatings is characterized by the nanocrystalline microstructure being a mixture of MgO, MgF_2, and $KMgF_3$, with the fluoride phases prevailing over magnesium oxide. MgO is uniformly dispersed throughout the MgF_2 matrix in the form of ultrafine grains, while $KMgF_3$ was confirmed in outer parts of the fabricated coating.
- Electrochemical tests showed a significant improvement in the corrosion resistance of the coated alloy as compared with bare material. The decrease in corrosion current density from 5.1×10^{-5} A/cm^2 to 9.32×10^{-6} A/cm^2 and the increase in polarization resistance from 340 Ω to 3428 Ω indicate effective surface passivation achieved through the conversion coating.
- Hydrogen evolution tests revealed a substantial reduction in H_2 release from the coated sample, in contrast to the uncoated material. This confirms the protective performance of the coating under simulated physiological conditions and its potential for application in implantology.

The novelty of the work lies in developing a low-cost and high-efficiency method of producing a conversion coating using a KOH+KF electrolyte and a simple technological setup, which effectively reduces hydrogen evolutio and protects the material from rapid degradation.

The application of the presented method provides the most balanced solution in terms of industrial feasibility. It ensures adequate corrosion resistance and biocompatibility while minimising process complexity, energy demand, and safety risks. Thus, constitutes a highly promising technique for the surface modification of biodegradable magnesium alloys intended for biomedical applications.

Acknowledgement

Research was carried out as part of the "Implementation Doctorate" program of the Ministry of Education and Science in Poland project No DWD/5/0007/2021

REFERENCES

[1] M. Hussain, S.M. Khan, K. Al-Khaled, M. Ayadi, N. Abbas, W. Chammam, Performance analysis of biodegradable materials for orthopedic applications. Mater. Today Commun. **31**, 103167 (2022).
DOI: https://doi.org/10.1016/j.mtcomm.2022.103167

[2] C. Liu, Z. Ren, Y. Xu, S. Pang, X. Zhao, Y. Zhao, Biodegradable magnesium alloys developed as bone repair materials: a review. Scanning 2018, 9216314 (2018).
DOI: https://doi.org/10.1155/2018/9216314

[3] D. Vojtěch, J. Kubásek, J. Čapek, Comparative mechanical and corrosion studies on magnesium, zinc and iron alloys as biodegradable metals. Mater. Tehnol. **49** (6), 877-882 (2015). DOI: https://doi.org/10.17222/mit.2014.129

[4] X. Gu, Y. Zheng, Y. Cheng, S. Zhong, T. Xi, In vitro corrosion and biocompatibility of binary magnesium alloys. Biomaterials **30** (4), 484-498 (2009). DOI: https://doi.org/10.1016/j.biomaterials.2008.10.021

[5] H. Li, J. Wen, Y. Liu, J. He, H. Shi, P. Tian, Progress in Research on Biodegradable Magnesium Alloys: A Review. Adv. Eng. Mater. **22**, 2000213 (2020). DOI: https://doi.org/10.1002/adem.202000213

[6] M.P. Staiger, A.M. Pietak, J. Huadmai, G. Dias, Magnesium and its alloys as orthopedic biomaterials: A review. Biomaterials **27** (9), 1728-1734 (2006). DOI: https://doi.org/10.1016/j.biomaterials.2005.10.003

[7] S. Lesz, B. Hrapkowicz, M. Karolus, K. Gołombek, Characteristics of the Mg-Zn-Ca-Gd alloy after mechanical alloying. Materials **14** (1), 226 (2021). DOI: https://doi.org/10.3390/ma14010226

[8] X. Wang, Y. Yu, L. Ji, Z. Geng, J. Wang, C. Liu, Calcium phosphate-based materials regulate osteoclast-mediated osseointegration. Bioact. Mater. **6** (12), 4517-4530 (2021). DOI: https://doi.org/10.1016/j.bioactmat.2021.05.003

[9] N. Luginin, A. Eroshenko, M. Khimich, K. Prosolov, A. Kashin, P. Uvarkin, A. Tolmachev, I. Glukhov, A. Panfilov, Y. Sharkeev, Severe plastic deformation of Mg–Zn–Zr–Ce alloys: Advancing corrosion resistance and mechanical strength for medical applications. Metals **13** (11), 1847 (2023). DOI: https://doi.org/10.3390/met13111847

[10] Y. Xiong, Q. Hu, R. Song, X. Hu, LSP/MAO composite biocoating on AZ80 magnesium alloy for biomedical application. Mater. Sci. Eng. C **75**, 1299-1304 (2017). DOI: https://doi.org/10.1016/j.msec.2017.03.003

[11] S.S. Saji, T.S.N. Sankara Narayanan, X. Chen, Conversion Coatings for Magnesium and its Alloys. Springer, Cham (2022). DOI: https://doi.org/10.1007/978-3-030-89976-9

[12] C.Y. Zhai, C.Y. Dai, X. Lv, B. Shi, Y.R. Li, Y. Yang, D. Fan, E.-S. Lee, Y. Sun, H.B. Jiang, Fluoride coatings on magnesium alloy implants. Bioinorg. Chem. Appl. 2022, 7636482 (2022). DOI: https://doi.org/10.1155/2022/7636482

[13] Y. Zhang, J.Y. Dai, L. Zhao, L.P. Wu, Corrosion resistance and biocompatibility of the $KMgF_3$ coated AZ31 magnesium alloy. J. Alloys Compd. **968**, 172210 (2023). DOI: https://doi.org/10.1016/j.jallcom.2023.172210

[14] Y. Zhang, Y. Guo, P. Zhou, T. Zhang, F. Wang, L. Chen, A plasma electrolytic oxidation coating on high purity Mg with excellent long term degradation performance and biocompatibility. Surf. Coat. Technol. **493**, 131236 (2024). DOI: https://doi.org/10.1016/j.surfcoat.2024.131236

[15] S. Hariprasad, S. Gowtham, S. Arun, M. Ashok, N. Rameshbabu, Fabrication of duplex coatings on biodegradable AZ31 magnesium alloy by integrating cerium conversion (CC) and plasma electrolytic oxidation (PEO) processes. J. Alloys Compd. **722**, 698-715 (2017). DOI: https://doi.org/10.1016/j.jallcom.2017.06.119

[16] M. Razavi, M. Fathi, O. Savabi, B. Hashemi Beni, D. Vashaee, L. Tayebi, Nanostructured merwinite bioceramic coating on Mg alloy deposited by electrophoretic deposition. Ceram. Int. **40** (7, Part A), 9473-9484 (2014). DOI: https://doi.org/10.1016/j.ceramint.2014.02.020

[17] M. Liang, C. Zhang, Z. Zhang, G. Chen, Corrosion resistance of W–Cr–C coatings fabricated by spark plasma sintering on tungsten matrix. Surf. Coat. Technol. **258**, 11-17 (2014). DOI: https://doi.org/10.1016/j.surfcoat.2014.06.012

[18] T. Li, Z. Datson, N. Darwish, Formation of organic monolayers on KF-etched Si surfaces. Surfaces. 7 (**2**), 358-368 (2024). DOI: https://doi.org/10.3390/surfaces7020022

[19] K. Anselme, Osteoblast adhesion on biomaterials. Biomaterials **21** (7), 667-681 (2000). DOI: https://doi.org/10.1016/S0142-9612(99)00242-2

[20] P. Tian, F. Peng, D. Wang, X. Liu, Corrosion behavior and cytocompatibility of fluoride incorporated plasma electrolytic oxidation coating on biodegradable AZ31 alloy. Regen. Biomater. **4** (1), 1-10 (2017). DOI: https://doi.org/10.1093/rb/rbw036

[21] H. Hornberger, S. Virtanen, A.R. Boccaccini, Biomedical coatings on magnesium alloys – a review. Acta Biomater. **8** (7), 2442-2455 (2012). DOI: https://doi.org/10.1016/j.actbio.2012.04.012

[22] P. Mohan Sathyaraj, K. Ravichandran, T.S.N. Sankara Narayanan, Controlling the rate of degradation of Mg using magnesium fluoride and magnesium fluoride–magnesium phosphate duplex coatings. J. Magnes. Alloys **10**, 295-312 (2021). DOI: https://doi.org/10.1016/j.jma.2021.06.005

[23] G.L. Song, Control of biodegradation of biocompatible magnesium alloys. Corros. Sci. **49** (4), 1696-1701 (2007). DOI: https://doi.org/10.1016/j.corsci.2007.01.001

[24] N.T. Kirkland, N. Birbilis, M.P. Staiger, Assessing the corrosion of biodegradable magnesium implants: a critical review of current methodologies and their limitations. Acta Biomater. **8** (3), 925-936 (2012). DOI: https://doi.org/10.1016/j.actbio.2011.11.014